Modeling Torques in Systems with Spin-Orbit Coupling

Nils Petter Jørstad[1,2], Wolfgang Goes[3], Siegfried Selberherr[2], and Viktor Sverdlov[1,2]
[1] Christian Doppler Laboratory for Nonvolatile Magnetoresistive Memory and Logic at the
[2] Institute for Microelectronics, TU Wien, Gußhausstraße 27-29, A-1040 Wien, Austria
[3] Silvaco Europe Ltd., Compass Point, St Ives, PE27 5JL, Cambridge, United Kingdom

We generalize the description of transport in ferromagnetic systems using a coupled spin and charge drift-diffusion approach to account for the spin-orbit torques acting on the magnetization. We consider both bulk and interfacial spin-orbit coupling and treat the transverse spin transport in the bulk of ferromagnets. We compare our approach with the typical assumption that the transverse spin currents are instantaneously absorbed in the ferromagnet. Furthermore, we investigate the effects of a strong interfacial Rashba spin-orbit coupling on the thickness and angular dependence of the torques, and we demonstrate its importance in capturing the behavior reported by experiments in the literature.

***Index Terms*—Spin and charge drift-diffusion, spin Hall effect, Rashba-Edelstein effect, spin-orbit torque.**

I. Introduction

SPIN-ORBIT torque (SOT) provides a fast and efficient way to manipulate the magnetization in devices such as magnetoresistive random access memory [1]. These devices take advantage of the strong spin-orbit coupling (SOC) in the bulk or at the interfaces of heavy metal (HM) layers to generate spin-polarized currents. The spin currents are injected into an adjacent ferromagnetic (FM) layer, where through spin dephasing the spins align with the magnetization while exerting a torque on the magnetization. In the bulk, the spin currents are generated through the spin Hall effect (SHE), which generates out-of-plane spin currents with in-plane polarization. The HM/FM interface plays a crucial role in the resulting torques as spin-flip scattering can be strong and additional spin currents can be generated through the Rashba-Edelstein effect (REE) at the interface [2]. Typically, the SOTs are modeled by assuming that the spins instantly align with the magnetization in the FM layer. In this picture, the SOT is determined purely by the spin current on the HM side of the interface, and the interface scattering is captured by the complex spin-mixing conductance [3].

In this work, we present a comprehensive approach to computing the spin torques in ferromagnetic systems with SOC. We compare the approach of assuming instant absorption of transverse spin currents in FM layers with one that allows for transmission of the transverse spin currents into the bulk by introducing a spin-mixing conductance for transmission. Furthermore, we explore the addition of the REE by considering spin-flip scattering from a Rashba SOC potential at the interface.

II. Coupled Spin and Charge Drift-Diffusion

The spin drift-diffusion model was first derived from the Boltzmann equation by Valet and Fert [4]. This model provides an efficient and less computationally demanding approach for exploring the transport in magnetoelectronic systems and has been shown to agree well with the more rigorous Boltzmann equation even at diffusion lengths close to the mean free path [5].

Corresponding author: N.P. Jørstad (email: jorstad@iue.tuwien.ac.at).

The spin polarization and charge current densities in HM and FM layers can be expressed as follows [6], [7]:

$$\tilde{J}_s = -\sigma\nabla\boldsymbol{\mu_s} + \beta_\sigma\sigma(\nabla\mu_c)\otimes\hat{\boldsymbol{M}} + \theta_{\mathrm{SHA}}\sigma\varepsilon\nabla\mu_c \quad (1)$$

$$\boldsymbol{J_c} = -\sigma\nabla\mu_c + \beta_D\sigma(\nabla\boldsymbol{\mu_s})\hat{\boldsymbol{M}} + \theta_{\mathrm{SHA}}\sigma\nabla\times\boldsymbol{\mu_s} \quad (2)$$

The spin polarization current density tensor $(\tilde{J}_s)_{ij}$ describes the flow of spin angular momentum in direction i with polarization j; it is expressed here in units of A/m^2. From here onward we will refer to $\tilde{J}_s$ simply as the spin current. The spin current can be converted back to units of angular momentum current density (J/m^2) by multiplication with $\hbar/2e$, where $\hbar$ and e are the reduced Plank constant and the elementary charge, respectively. μ_c is the chemical potential, while $\boldsymbol{\mu_s}$ is the spin chemical potential proportional to the spin accumulation $\boldsymbol{\mu_s} = (D_e/\sigma)(e/\mu_B)\boldsymbol{S}$. σ, D_e, and μ_B are the electrical conductivity, the electron diffusion constant, and the Bohr magnetron, respectively. $\hat{\boldsymbol{M}}$ is the direction of the magnetization. β_σ and β_D are the dimensionless conductivity and diffusion polarizations, respectively. The magnitude of the direct and inverse SHE is captured by the spin Hall angle θ_{SHA}, while its orthogonal flow and polarization directions are described by the unit antisymmetric tensor ε_{ijk} [8]. Other bulk spin-orbit effects, such as the magnetic spin Hall effect or the anomalous Hall effect, can be included in equation (1) to enhance the model even further.

For a steady state, the chemical potentials are determined by the continuity equations for spin and charge [6], [7]:

$$\nabla\tilde{J}_s = -\sigma\left(\frac{\boldsymbol{\mu_s}}{\lambda_{sf}^2} + \frac{\boldsymbol{\mu_s}\times\hat{\boldsymbol{M}}}{\lambda_J^2} + \frac{\hat{\boldsymbol{M}}\times(\boldsymbol{\mu_s}\times\hat{\boldsymbol{M}})}{\lambda_\phi^2}\right) \quad (3)$$

$$\nabla\cdot\boldsymbol{J_c} = 0 \quad (4)$$

λ_{sf}, λ_J, and λ_ϕ are the spin-flip, spin exchange, and spin dephasing lengths, respectively.

At external boundaries not containing contacts, we assume vanishing flux of spin and charge, i.e. $\boldsymbol{J_c}\cdot\boldsymbol{n} = 0$ and $J_s\boldsymbol{n} = 0$.

At external boundaries containing contacts, Dirichlet boundary conditions for the electrical potential are applied, and the contacts are kept long to ensure the total decay of the spin chemical potential.

III. Boundary Conditions for HM/FM interfaces

We consider an interface at $z = 0$ with an HM and FM layer below and above the interface, respectively. At the interface, we assume a spin-independent scattering potential, an interfacial exchange interaction, and an interfacial Rashba SOC:

$$V(\boldsymbol{r}) = \frac{\hbar^2 k_F}{m_e}\delta(z)\Big[u_0 I_{2\times 2} + \boldsymbol{\sigma}\cdot\left(u_{ex}\hat{\boldsymbol{M}} + u_R\hat{\boldsymbol{z}}\times\frac{\boldsymbol{k}}{k_F}\right)\Big] \quad (5)$$

u_0, u_{ex}, and u_R are the dimensionless magnitudes of the spin-independent potential, the exchange interaction, and the Rashba SOC at the interface, respectively. $\delta(z)$ is the Dirac delta function, k_F is the Fermi wave number, and m_e is the electron mass. $\boldsymbol{\sigma}$ is the vector of Pauli matrices and $\boldsymbol{k}$ is the wave vector. By considering plane-wave scattering from the interface potential one can derive scattering matrices for reflection and transmission $R_{\alpha\beta}(\boldsymbol{k})$, and $T_{\alpha\beta}(\boldsymbol{k})$, respectively, describing an ensemble of spins with polarization β being scattered into polarization α [2], [9], [10], with indices $\alpha,\beta\in\{x,y,z,c\}$, where x,y,z denote the spin polarization directions and c denotes the charge. The same matrices can be used as boundary conditions for the Boltzmann equation, to describe the scattering of an incident spin and charge density function $g^I_\alpha(0^\pm,\boldsymbol{k})$ from the interface. $0^\pm$ denotes if the density function at the interface is incident from the upper $(+)$ or lower $(-)$ side of the interface. The spin and charge currents above and below the interface are then described by [2]:

$$J_{z\alpha}(0^\pm) = \mp\frac{e}{\hbar(2\pi)^3}\int_{\mathrm{FS}} d\boldsymbol{k}\frac{k_z}{k_F}\big[(\delta_{\alpha\beta}-R_{\alpha\beta}(\boldsymbol{k}))g^I_\beta(0^\pm,\boldsymbol{k}) - T_{\alpha\beta}(\boldsymbol{k})g^I_\beta(0^\mp,\boldsymbol{k})\big] \quad (6)$$

$\delta_{\alpha\beta}$ is the Kronecker delta; the integration is performed over the incident part of the Fermi surface and a summation convention is assumed for repeated indices.

We consider two contributions to the incident distribution function which are isotropic and anisotropic in k-space. The isotropic contribution captures the contribution of incident charge/spin currents and is described by the charge/spin chemical potentials in the HM and FM layers. The anisotropic contribution captures the shift of the distribution function due to an applied electric field along x [2], [11]:

$$g^I_\alpha(0^\pm,\boldsymbol{k}) = e\mu_\alpha(0^\pm) + e\Delta\mu^E_\alpha(\boldsymbol{k},0^\pm) \quad (7)$$

In the relaxation time approximation the shift is given by $\Delta\mu^E_\alpha(\boldsymbol{k},0^\pm) = \hbar k_x\tau^\pm P^\pm_\alpha E_{\mathrm{ip}}/m_e$, where $\tau^\pm$ and $P^\pm_\alpha$ are the momentum relaxation times and the dimensionless charge/spin polarization at either side of the interface, respectively. $E_{\mathrm{ip}} = E_x(0)$ is the magnitude of the applied in-plane electric field at $z = 0$.

After inserting (7) into (6) and performing the integration, the spin and charge currents can then be expressed as

$$\check{\boldsymbol{J}}_{\boldsymbol{z}}(0^\pm) = \pm\left[\overline{G}\check{\boldsymbol{\mu}}(0^\pm) - \overline{\Gamma}\check{\boldsymbol{\mu}}(0^\mp)\right] + \check{\boldsymbol{\sigma}}^\pm E_{\mathrm{ip}}, \quad (8)$$

where $\check{\boldsymbol{J}}_{\boldsymbol{z}}(0^\pm) = [\boldsymbol{J}_{\boldsymbol{sz}}(0^\pm), J_{cz}(0^\pm)]$ and $\check{\boldsymbol{\mu}}(0^\pm) = [\boldsymbol{\mu}_{\boldsymbol{s}}(0^\pm), \mu_c(0^\pm)]$ are four component current and potential vectors, respectively, for spin and charge. $\overline{G}$ and $\overline{\Gamma}$ are interface conductance tensors of rank 4, and $\check{\boldsymbol{\sigma}}^\pm$ are the conductivity vectors at either side of the interface. $\overline{G}$ is related to the complex spin-mixing conductance from magnetoelectronic circuit theory, while $\overline{\Gamma}$ contains the mixing conductances for transmission to capture the spin currents from transmitted spins [2], [9], [12]. In magnetoelectronic circuit theory, it is assumed that the transverse spins dephase rapidly in the FM layer and, consequently, that the transverse spin current and accumulation are instantaneously absorbed in the FM layer. This approximation is obtained by neglecting the transverse components of the spin current on the FM side of the interface, i.e. $\boldsymbol{J}^\perp_{\boldsymbol{sz}}(0^+) = [I_{3\times3} - \hat{\boldsymbol{M}}\otimes\hat{\boldsymbol{M}}]\boldsymbol{J}_{\boldsymbol{sz}}(0^+) = 0$, where $[I_{3\times3}-\hat{\boldsymbol{M}}\otimes\hat{\boldsymbol{M}}]$ is an operator which removes the longitudinal spin component.

IV. Spin Torques

The spin torques acting on the magnetization in the bulk of FM layers are given by the transfer of angular momentum from the spin accumulation through exchange-induced precession and spin dephasing, described by the second and third term contributing to the divergence of the spin current in equation (3) [6], [7]. The total spin torque acting on the magnetization in the bulk is then obtained by integration over the volume of the ferromagnetic layer:

$$\boldsymbol{\mathcal{T}}^{\mathbf{FM}}_{\boldsymbol{s}} = -\frac{\sigma}{A}\int_{\mathrm{FM}} d\boldsymbol{x}\left(\frac{\boldsymbol{\mu_s}\times\hat{\boldsymbol{M}}}{\lambda_J^2} + \frac{\hat{\boldsymbol{M}}\times(\boldsymbol{\mu_s}\times\hat{\boldsymbol{M}})}{\lambda_\phi^2}\right) \quad (9)$$

A is the area of the HM/FM interface.

At the interface the torque is obtained from the exchange interaction between the magnetization and the spin density at the interface $\boldsymbol{s_0}$ [9], [11]:

$$\boldsymbol{\mathcal{T}}^{\mathbf{int}}_{\boldsymbol{s}} = -e\int_{0^-}^{0^+} dz\frac{J_{ex}}{\hbar}\boldsymbol{s_0}\times\hat{\boldsymbol{M}} \quad (10)$$

$J_{ex} = -\hbar^2 k_F u_{ex}\delta(z)/m_e$ is the exchange energy at the interface. Using the transmission matrix to compute the spin density at the interface one obtains [11]:

$$\mathcal{T}^{\mathrm{int}}_\alpha = \frac{u_{ex}e}{\hbar(2\pi)^3}\int_{\mathrm{FS}} d\boldsymbol{k}\varepsilon_{\alpha ij}\hat{M}_i T_{j\beta}(\boldsymbol{k})\big[g^I_\beta(0^+,\boldsymbol{k}) + g^I_\beta(0^-,\boldsymbol{k})\big], \quad (11)$$

where the indices go only over the spin polarization components, i.e. $\alpha,\beta,i,j\in\{x,y,z\}$. Inserting (7) into (11) yields:

$$\boldsymbol{\mathcal{T}}^{\mathbf{int}}_{\boldsymbol{s}} = \tilde{\Gamma}^{\mathrm{int}}_s\left[\boldsymbol{\mu_s}(0^-) + \boldsymbol{\mu_s}(0^+)\right] + \boldsymbol{\gamma}^{\mathbf{int}}_{\boldsymbol{s}}E_{\mathrm{ip}} \quad (12)$$

$\tilde{\Gamma}^{\mathrm{int}}_s$ is the rank 3 interface torkance tensor and $\boldsymbol{\gamma}^{\mathbf{int}}_{\boldsymbol{s}}$ is the interface torkivity vector [9].

This article has been accepted for publication in IEEE Transactions on Magnetics. This is the author's version which has not been fully edited and content may change prior to final publication. Citation information: DOI 10.1109/TMAG.2025.3525810

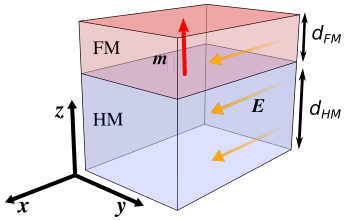

Fig. 1. A sketch of a HM($d_{\rm HM}$)/FM($d_{\rm FM}$) bilayer with an applied electric field along x. The magnetization points along z.

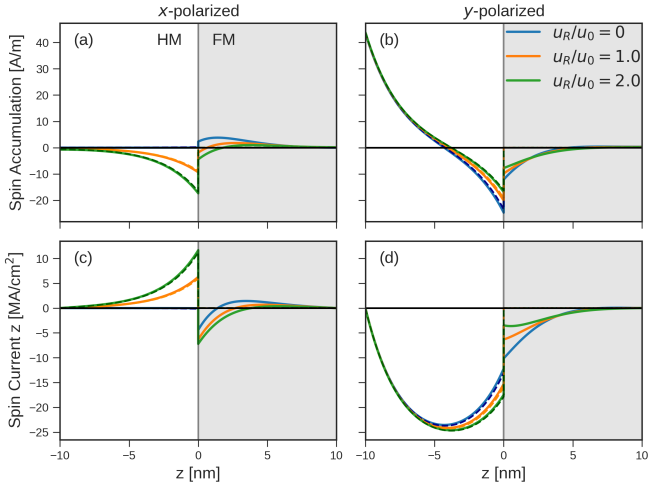

Fig. 2. The transverse spin accumulation and spin current in the HM(10 nm)/FM(10 nm) bilayer depicted in Fig. 1. The upper row shows the spin accumulations and the lower row shows the spin currents, while the left and right columns show the results for x and y polarization, respectively. Dashed lines are obtained by assuming instant absorption of transverse spin in the FM.

Assuming the transverse spin current is instantly absorbed in the FM $\boldsymbol{\mathcal{T}}_{\boldsymbol{s}}^{\mathbf{FM}} = \boldsymbol{J}_{\boldsymbol{sz}}^{\perp}(0^+)$ together with $\boldsymbol{\mu}_{\boldsymbol{s}}^{\perp}(0^+) = 0$, the total spin torque can be expressed as follows [11]:

$$\boldsymbol{\mathcal{T}}_{\boldsymbol{s}}^{\mathbf{tot}} = \left(\tilde{\Gamma}_{s}^{\rm int} + \tilde{\Gamma}_{s}^{\rm FM}\right)\boldsymbol{\mu}_{\boldsymbol{s}}(0^-) + \left(\boldsymbol{\gamma}_{\boldsymbol{s}}^{\mathbf{int}} + \boldsymbol{\gamma}_{\boldsymbol{s}}^{\mathbf{FM}}\right) E_{\rm ip} \quad (13)$$

$\boldsymbol{\gamma}_{\boldsymbol{s}}^{\mathbf{FM}} = [I_{3\times3} - \hat{\boldsymbol{M}} \otimes \hat{\boldsymbol{M}}]\boldsymbol{\sigma}_{\boldsymbol{s}}^{+}$ is the bulk torkivity vector and $\tilde{\Gamma}_{s}^{\rm FM} = \tilde{\Gamma}_{s}[I_{3\times3} - \hat{\boldsymbol{M}} \otimes \hat{\boldsymbol{M}}]$ is the bulk torkance tensor [9]. The torques can be converted from units of current density into units of magnetization flux density by multiplication with $-g_e\mu_B/e$, where g_e is the electron g-factor.

V. Results & Discussion

We consider an HM/FM bilayer, depicted in Fig. 1, with a 10^6 V/m applied electric field along x and solve the drift-diffusion equation using the boundary conditions. We assume a spin Hall effect with $\theta_{\rm SHA} = 6\%$ in the HM layer and varying strengths of interfacial SOC u_R at the HM/FM interface. The resulting transverse spin accumulation and spin currents in the bilayer are shown in Fig. 2. The solid lines show the results obtained by considering the decay of the transverse spin currents in the bulk of the FM layer, while the dashed lines show the result obtained with the approximation that the transverse spin currents are instantaneously absorbed at the FM side of the interface. We observe a good match between the two approaches in the HM layer, while in the FM layer,

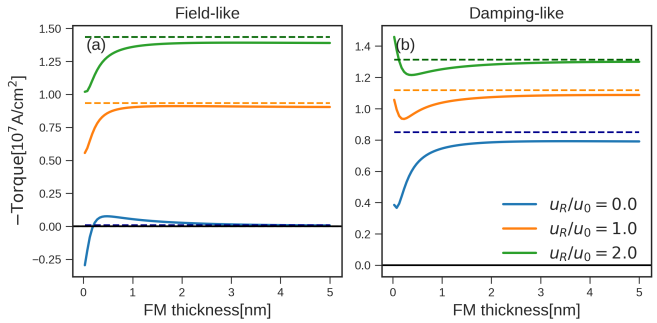

Fig. 3. The total spin torque acting on the magnetization of the FM layer, for the system depicted in Fig. 1, as a function of the upper FM thickness $d_{\rm FM}$. The HM thickness is kept at 4 nm. Dashed lines are obtained by assuming instant absorption of transverse spin in the FM. Panel (a) shows the field-like torque and panel (b) shows the damping-like torque.

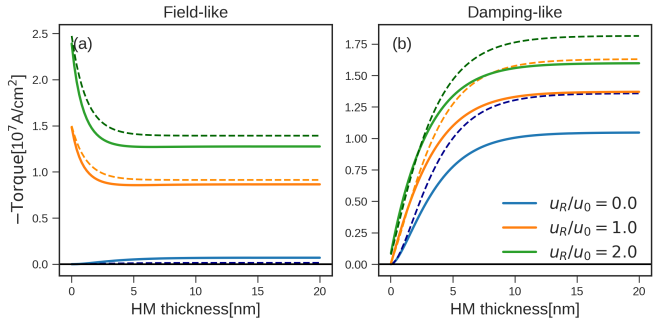

Fig. 4. Same as Fig. 3, except that the HM layer thickness is varied, and the FM layer thickness is kept at 0.5 nm.

there are no transverse spin currents present using this approximation and the transverse spin transport is only captured by the full model. At the interface, there is a discontinuity of the spin accumulation and current corresponding to the spin current transferred to the magnetization at the interface due to the interfacial exchange interaction. For $u_R \neq 0$, part of the spin current is also transferred to the crystal lattice through the precession of the spin density around the interfacial spin-orbit field, which does not contribute to the spin torque.

To investigate the validity of the instant transverse spin decay approximation, we vary the FM layer thickness and compute the total torque acting on the layer using the two models. We decompose the spin torques into field-like and damping-like contributions, i.e. $\boldsymbol{\mathcal{T}}_{\boldsymbol{s}} = \mathcal{T}_f\hat{\boldsymbol{f}} + \mathcal{T}_d\hat{\boldsymbol{d}}$, which for an SOT bilayer system are along $\hat{\boldsymbol{f}} = \hat{\boldsymbol{M}} \times (\hat{\boldsymbol{z}} \times \hat{\boldsymbol{E}})$ and $\hat{\boldsymbol{d}} = \hat{\boldsymbol{M}} \times [\hat{\boldsymbol{M}} \times (\hat{\boldsymbol{z}} \times \hat{\boldsymbol{E}})]$, respectively [2]. The resulting torques can be seen in Fig. 3. We observe that the two approaches agree well for a thick FM layer as all of the transverse spin current is transferred to the magnetization. The minor difference between the models in this thickness regime originates from the contribution of the transverse spin accumulation at the FM side of the interface to the spin current at the HM side of the interface, which is not captured by the reduced model. In the limit of $\lambda_\phi \to 0$, the reduced model is re-obtained from the full model. For a thin FM layer, the two approaches disagree as in the full model, the spin current is not entirely absorbed in the FM layer and is instead partly reflected back into the HM layer.

In Fig. 4 we show the dependence of the torques on the

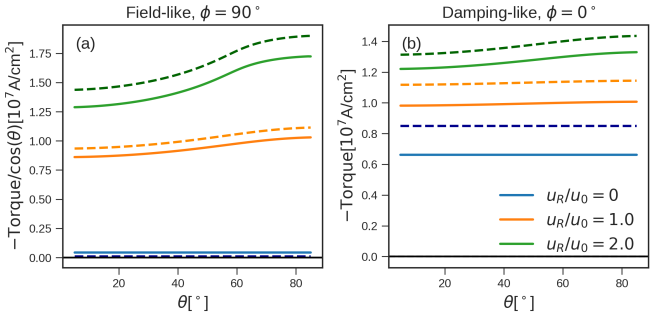

Fig. 5. Same as Figs. 3 and 4, except that the polar angle of the magnetization direction θ is varied and the FM and HM layer thicknesses are kept at 4 nm and 0.5 nm, respectively. In panels (a) and (b) the azimuthal angle ϕ is kept at 90° and 0°, respectively. The field-like torque is divided by $\cos(\theta)$ to remove the conventional angular dependence and highlight the effects of interfacial SOC.

HM layer thickness. The two approaches give qualitatively similar results, therefore, the instant absorption assumption with proper parameter fitting can be a good approximation for bilayer systems. The addition of the REE yields a much stronger field-like torque which does not vanish with decreasing HM layer thickness in agreement with reported experimental results [13].

The dependence of the torques on the magnetization direction is typically entirely described by $\hat{\boldsymbol{d}}$ and $\hat{\boldsymbol{f}}$, however, with interfacial SOC more complex dependencies are allowed due to the interplay between the SOC and exchange interaction at the interface. We express the magnetization direction in terms of the polar and azimuthal angles $\hat{\boldsymbol{M}}(\theta,\phi) = [\cos(\phi)\sin(\theta), \sin(\phi)\sin(\theta), \cos(\theta)]$. For $\phi = 0$ the damping-like torque will have a constant dependence on θ and for $\phi = 0^\circ$ the field-like torque will have a $\cos(\theta)$ dependence. Fig. 5 shows the dependence of the field-like and damping-like torque on the polar angle in the two planes given by $\phi = 90^\circ$ and $\phi = 0$, respectively. We observe that for zero interfacial SOC the angular dependence is fully described by $\hat{\boldsymbol{d}}$ and $\hat{\boldsymbol{f}}$, while for increasingly stronger u_R the angular dependence becomes more complex, implying that the magnitudes of the field-like and damping-like torques depend on $\hat{\boldsymbol{M}}$, i.e. $\mathcal{T}_f(\hat{\boldsymbol{M}})$ and $\mathcal{T}_d(\hat{\boldsymbol{M}})$. This additional angular dependence has been thoroughly reported in HM/FM SOT systems [14], [15], and can be explained in terms of so-called higher-order contributions to the torque. By not taking the crystal structure into account, the contributions to the torque allowed by the continuous rotational symmetries of the HM/FM bilayer structure are described by

$$\boldsymbol{\mathcal{T}_s} = \sum_{l=0}^{\infty} (M_z)^{2l} \big[a_l(\hat{\boldsymbol{z}} \times \hat{\boldsymbol{E}}) \times \hat{\boldsymbol{M}} + b_l \hat{\boldsymbol{M}} \times [(\hat{\boldsymbol{z}} \times \hat{\boldsymbol{E}}) \times \hat{\boldsymbol{M}}] + c_l(\hat{\boldsymbol{M}} \cdot \hat{\boldsymbol{E}})\hat{\boldsymbol{z}} \times \hat{\boldsymbol{M}} + d_l(\hat{\boldsymbol{M}} \cdot \hat{\boldsymbol{E}})\hat{\boldsymbol{M}} \times (\hat{\boldsymbol{z}} \times \hat{\boldsymbol{M}}) \big], \quad (14)$$

where a_l, b_l, c_l, and d_l are expansion coefficients [2], [14], [15]. The first two terms for $l = 0$ are the typical field-like and damping-like terms, the latter two explain the angular dependence observed in the damping-like torque for $\phi = 0^\circ$. For the field-like torque in the $\phi = 90^\circ$ plane, $l > 0$ contributions from the first two terms are required to obtain the additional observed angular dependence. With the generalized boundary conditions presented in this work, these higher-order contributions are included as a phenomenological consequence of the interfacial SOC.

VI. Conclusions

A generalized coupled charge and spin drift-diffusion approach for computing spin torques in ferromagnetic structures with SOC has been presented. Interfacial SOC is accounted for through boundary conditions derived by considering scattering from a Rashba interface potential. We treat the transverse spin inside ferromagnets and show that the typical approximation that the transverse spin currents are instantly absorbed inside FM layers, agrees qualitatively with the full treatment. Moreover, our results show that the inclusion of interfacial Rashba SOC is crucial for capturing the thickness and angular dependence of the SOTs reported in experiments.

Acknowledgment

The financial support by the Federal Ministry of Labour and Economy, the National Foundation for Research, Technology and Development, and the Christian Doppler Research Association is gratefully acknowledged. The authors acknowledge TU Wien Bibliothek for financial support through its Open Access Funding Program.

References

[1] S. Hu, X. Qiu, C. Pan, W. Zhu, Y. Guo, D.-F. Shao, Y. Yang, D. Zhang, and Y. Jiang, "Frontiers in all electrical control of magnetization by spin orbit torque," *J. Phys. Condens. Matter.*, vol. 36, no. 25, p. 253001, 2024.

[2] V. P. Amin, P. M. Haney, and M. D. Stiles, "Interfacial spin–orbit torques," *J. of Appl. Phys.*, vol. 128, no. 15, p. 151101, 2020.

[3] A. Brataas, G. E. W. Bauer, and P. J. Kelly, "Non-collinear magnetoelectronics," *Phys. Rep.*, vol. 427, no. 4, pp. 157–255, 2006.

[4] T. Valet and A. Fert, "Theory of the perpendicular magnetoresistance in magnetic multilayers," *Phys. Rev. B*, vol. 48, pp. 7099–7113, 1993.

[5] D. R. Penn and M. D. Stiles, "Spin transport for spin diffusion lengths comparable to mean free paths," *Phys. Rev. B*, vol. 72, p. 212410, 2005.

[6] P. M. Haney, H.-W. Lee, K.-J. Lee, A. Manchon, and M. D. Stiles, "Current induced torques and interfacial spin-orbit coupling: Semiclassical modeling," *Phys. Rev. B*, vol. 87, p. 174411, 2013.

[7] S. Lepadatu, "Unified treatment of spin torques using a coupled magnetisation dynamics and three-dimensional spin current solver," *Sci. Rep.*, vol. 7, no. 1, p. 12937, 2017.

[8] M. I. Dyakonov, "Magnetoresistance due to edge spin accumulation," *Phys. Rev. Lett.*, vol. 99, p. 126601, 2007.

[9] V. P. Amin and M. D. Stiles, "Spin transport at interfaces with spin-orbit coupling: Phenomenology," *Phys. Rev. B*, vol. 94, p. 104420, 2016.

[10] N. P. Jørstad, S. Fiorentini, J. Ender, W. Goes, S. Selberherr, and V. Sverdlov, "Micromagnetic modeling of SOT-MRAM dynamics," *Phys. Rev. B Condens.*, vol. 676, p. 415612, 2024.

[11] V. P. Amin and M. D. Stiles, "Spin transport at interfaces with spin-orbit coupling: Formalism," *Phys. Rev. B*, vol. 94, p. 104419, 2016.

[12] N. P. Jørstad, W. Goes, S. Selberherr, and V. Sverdlov, "Spin drift-diffusion boundary conditions for fem modeling of multilayer SOT devices," in *International Conference on Simulation of Semiconductor Processes and Devices (SISPAD)*, 2023, pp. 1–4.

[13] A. Ghosh, K. Garello, C. O. Avci, M. Gabureac, and P. Gambardella, "Interface-enhanced spin-orbit torques and current-induced magnetization switching of $\text{Pd}/\text{Co}/\text{AlO}_x$ layers," *Phys. Rev. Appl.*, vol. 7, p. 014004, 2017.

[14] K. Garello, I. M. Miron, C. O. Avci, F. Freimuth, Y. Mokrousov, S. Blügel, S. Auffret, O. Boulle, G. Gaudin, and P. Gambardella, "Symmetry and magnitude of spin–orbit torques in ferromagnetic heterostructures," *Nat. Nanotechnol.*, vol. 8, no. 8, p. 587–593, 2013.

[15] E.-S. Park, D.-K. Lee, F. Xue, B.-C. Min, H. C. Koo, P. M. Haney, K.-W. Kim, and K.-J. Lee, "Strong higher-order angular dependence of spin-orbit torque in W/CoFeB bilayer," *Phys. Rev. B*, vol. 107, p. 064411, 2023.